IEEE Photonics Journal
An IEEE Photonics Society Publication

Comparison of Plasmonic Arrays of Holes Recorded by Interference Lithography and Focused Ion Beam

Volume 4, Number 2, April 2012

J. W. Menezes
L. A. M. Barea
E. F. Chillcce
N. Frateschi
L. Cescato

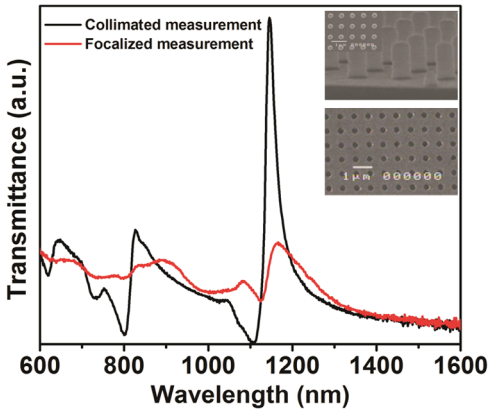

DOI: 10.1109/JPHOT.2012.2190497
1943-0655/$31.00 ©2012 IEEE

Comparison of Plasmonic Arrays of Holes Recorded by Interference Lithography and Focused Ion Beam

J. W. Menezes, L. A. M. Barea, E. F. Chillcce, N. Frateschi, and L. Cescato

Instituto de Física Gleb Wataghin, UNICAMP, 13083-970 Campinas SP, Brazil

DOI: 10.1109/JPHOT.2012.2190497
1943-0655/$31.00 ©2012 IEEE

Manuscript received January 14, 2012; revised February 24, 2012; accepted March 6, 2012. Date of publication March 9, 2012; date of current version April 10, 2012. This work was supported by the Conselho Nacional de Pesquisas (CNPq), the Fundação de Amparo a Pesquisa do Estado de São Paulo (FAPESP), and Fotônica para Comunicações Ópticas (FOTONICOM). Corresponding author: J. W. Menezes (e-mail: jacsonwm@uvic.ca).

Abstract: In this paper, we compare the geometric characteristics and the optical properties of plasmonic hole arrays recorded in gold (Au) films using two different techniques, namely, focused ion beam (FIB) and interference lithography (IL). The morphology of the samples was analyzed using a scanning electron microscope (SEM), and the plasmonic peaks were measured from the transmission spectrum of the samples. The diameters of the holes recorded by IL present approximately the same statistical deviation as those fabricated by FIB but in a much larger area. Although the transmittance measurements of both types of samples exhibit the characteristic plasmonic peaks, the intrinsic fabrication errors of each technique affect differently the optical spectra.

Index Terms: Lithography, interference, focused ion beam, plasmonics.

1. Introduction

Periodic arrays of nanoholes in metallic thin films present interesting properties such as extraordinary transmittance peaks [1], [2] and a strong local field enhancement in proximity of the holes [3], [4]. Such phenomena have been attributed to Surface Plasmon Resonances (SPR) [2], [5] that can be excited when the condition for momentum conservation

$$\vec{k}_{SP} = \vec{k}_{//} + \vec{G} \tag{1}$$

is achieved. $\vec{k}_{SP}$ is the wave-vector of the SP, $\vec{k}_{//}$ is the component of the incident light wave-vector parallel to the metal surface, and $\vec{G}$ is the array wave-vector. The modulus of such wave vectors are given, respectively, by

$$k_{SP} = k_0 \left(\frac{\epsilon_d \epsilon_m}{\epsilon_d + \epsilon_m} \right)^{1/2} \tag{2}$$

$$k_{//} = \frac{2\pi}{\lambda} sin\theta \tag{3}$$

$$G = \frac{2\pi}{\Lambda} \tag{4}$$

with ϵ_d being the dielectric constant of the surrounding medium, ϵ_m the dielectric constant of the metal, k_0 the wavenumber of the incident wave, θ the incident angle, and Λ the array period.

For normal incidence ($\vec{k}_{//} = 0$) and a square array of holes, the wavelength position of such resonance peaks is given by

$$\lambda_0 = \frac{\Lambda}{(i^2 + j^2)^{1/2}} \left(\frac{\epsilon_d \epsilon_m}{\epsilon_d + \epsilon_m} \right)^{1/2}. \quad (5)$$

Each pair of integers i and j represents an SP mode excited at the metal interface. It is common to have different dielectrics on each side of the metal film: the substrate that supports the metal film (ϵ_{subs}) and the upper medium in direct contact to the metal surface (ϵ_{air}). Thus, two different kinds of transmittance peaks are expected: due to the metal–air interface, and due to the metal–substrate, for each SP mode (i, j). Equation (5) shows a simple model of how to estimate the position of the resonance peaks. For more precise and complete calculation of this value, other parameters have to be considered. Previously works have shown that the hole shape [6], hole size [7] and film thickness [8], not considered in (5), have influence on the shape and position of the SPR peaks. Because these resonances are very sensitive to the surrounding media, these structures are promising for sensor applications [9], [10] and light manipulation [11]. Besides, the high local field generates a strong enhancement in light induced phenomena such surface enhanced Raman scattering (SERS) [12] and may be used to increase the efficiency in solar cells [13].

Although several techniques have been proposed to record plasmonic arrays [14]–[17], most of the arrays of nanoholes, for plasmonic applications, have been recorded with focused ion beam (*FIB*) milling [1]–[4], [7], [9], [12], [18]. FIB allows the precise fabrication of highly ordered arrays with well-defined geometry and hole size control. Also, FIB can be extremely useful for positioning different arrays on top of different structures of small sizes [19]. However, because of the serial nature of the FIB process, the time required to record high density arrays over large areas is usually excessive. Also, ion beam field limitation restricts this approach to plasmonic arrays typically smaller than 100 μm $\times$ 100 μm. For the generation of high-resolution periodic structures over large areas, the interference lithography (IL) [19]–[22] is an interesting and cheaper alternative. By using a double exposure of a photoresist film to the same interference pattern, large area 2-D arrays can be recorded [22]. In this paper, we compare the morphological characteristics and the optical properties of arrays of holes recorded in gold films using these two techniques.

2. Fabrication of the Arrays

2.1. Focused Ion Beam

For the hole arrays fabrication using the FIB technique, a glass substrate was cleaned, coated with 300 nm of SU-8, and covered with an Au film (100 nm thickness) using a Varian thermal evaporation system. SU-8 is employed to improve the adhesion between Au and glass. After that the film was patterned in a FIB model NOVA 200 Nanolab using the following conditions: 30 kV of voltage, 0.3 nA of current and an all time of etching of 45 s. Fig. 1 shows SEM micrographs of the recorded sample. Fig. 1(a) shows an overview of the whole 18 μm $\times$ 18 μm sample, while Fig. 1(b) shows the details of the holes recorded in the gold film.

2.2. Interference Lithography

For the hole array fabrication using the IL technique, a lift-off process was employed. The substrate is also glass coated with 300 nm of SU-8. Essentially, a photoresist template is first imprinted on the substrate using IL. A thin Au film is deposited and the photoresist removed with acetone. Fig. 2 shows the schematic sequence of the process. In order to record the template, the substrate is coated with a positive photoresist SC 1827 of 600 nm of thickness. The photoresist is exposed twice to the same interference fringe pattern rotating the sample of 90° between the exposures [22]. After the development in Microposit 351 Developer (Rohm and Haas), a square array of photoresist columns is formed, as can be seen in Fig. 3(a). The photoresist template is then coated with a thin Au film (100 nm thickness) by thermal evaporation in the same Varian system. Because of the high

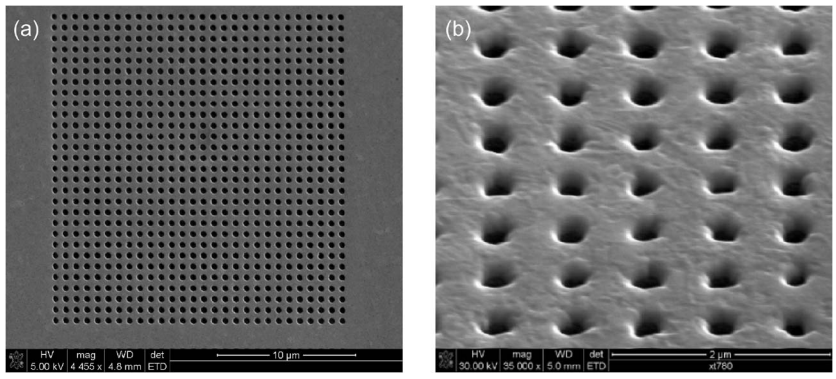

Fig. 1. (a) SEM micrography of the top view of the whole FIB sample (18 μm $\times$ 18 μm). (b) Higher magnification showing the detail of the holes.

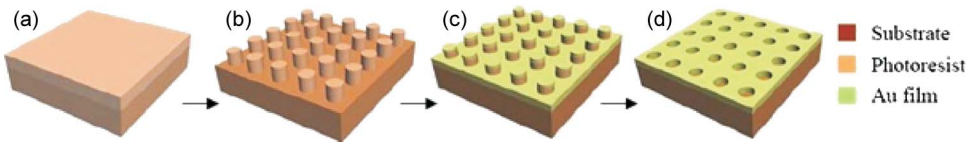

Fig. 2. Scheme of nanohole array fabrication. (a) Photoresist deposition by spin coating. (b) Double exposure of two-beam interference patterns using $\lambda = 458$ nm followed by photoresist development. (c) Au film deposition by thermal evaporation. (d) Lift-off of the photoresist template.

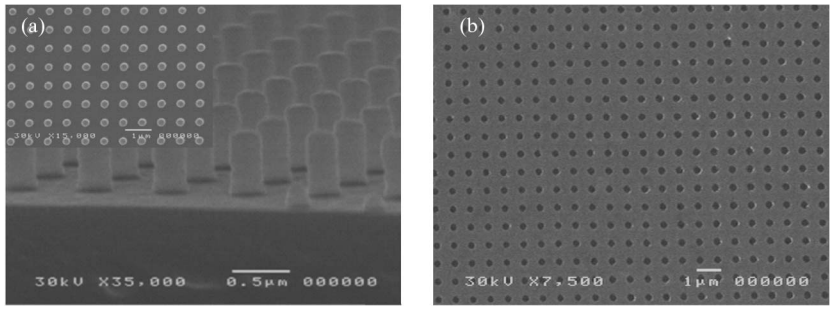

Fig. 3. (a) View of the photoresist template composed of a square array of photoresist columns. The inset shows a top view of the structure. (b) Top view of the array of holes obtained after the lift-off of the photoresist.

verticality of the photoresist columns and the directional nature of the Au deposition, lift-off is very efficient leaving the substrate patterned with the array of holes [see Fig. 3(b)].

3. Characterization of the Arrays

3.1. Morphologic Parameters of the Samples

The dimensions of the FIB and IL hole arrays were obtained from SEM top view micrographs at different regions of the samples. The FIB samples presented a periodic distance (between holes) of 700 nm with a standard deviation of 3 nm, while the IL samples presented a periodic distance of 675 nm with a standard deviation of 5 nm. For the hole diameter, however, we observe a larger deviation in the sizes. Fig. 4(a) shows the histogram of distribution of the hole diameters for the samples recorded by FIB. The hole diameter average (covering a 18 μm $\times$ 18 μm area) is 305 nm

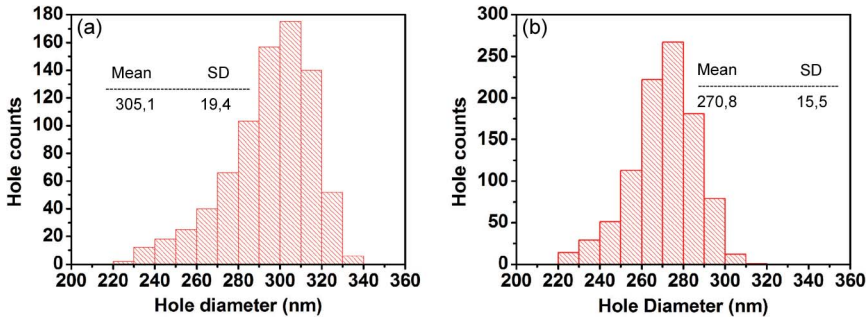

Fig. 4. Histogram of hole diameter of the arrays recorded by (a) FIB and (b) IL.

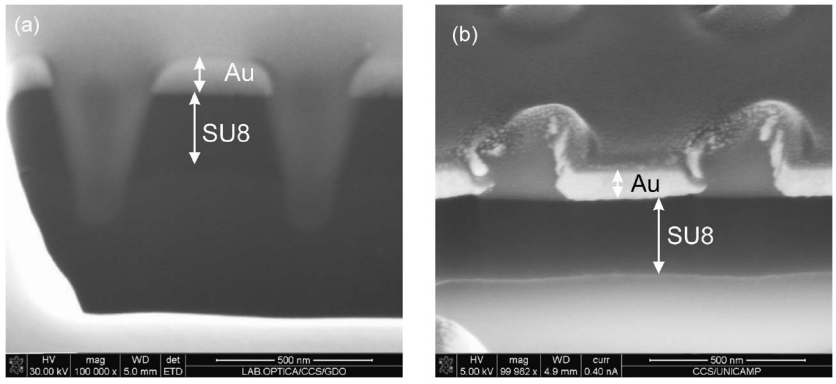

Fig. 5. Cross section of the samples recorded by (a) FIB and (b) IL.

with a standard deviation of 20 nm. Fig. 4(b) shows the corresponding histogram for the IL samples. In this case the hole diameter average (considering a region of 8 mm $\times$ 8 mm area) is 270 nm with a standard deviation of 15 nm. These deviations correspond to a variation rate (deviation/mean diameter) of 5.5% and 6.5% for the IL and FIB samples, respectively.

In order to study the details of the holes, both samples were prepared and analyzed using the FIB system. First, a 500-nm-thick film of Pt was deposited over the holes. This is done to protect the recorded structures and to improve the contrast. Subsequently, a rectangular section was milled in order to expose the cross section of the holes [23], [24]. Fig. 5(a) shows the high resolution SEM image of the cross section of the holes recorded by FIB, while Fig. 5(b) shows the corresponding image for the holes recorded by IL.

Note that in the case of FIB sample there is a strong conical milling of the substrate. This effect is more pronounced for larger holes diameters. Also, the top surface edge of the Au film is rounded, resulting in a variation of the hole diameter with the depth of the Au film. The hole diameter is about 15% larger on the top of the Au film than it is near the substrate. This conical shape of the milling occurs probably because of the longer exposure of the top of the sample to the Ga ions as well because of the Gaussian shape of the FIB. In Fig. 5(b), we note in the IL sample the presence of a burr on the edges of the hole. This burr can be clearly observed in the SEM image shown in Fig. 6. The burr results from the Au deposition on the lateral walls of the photoresist template that was not removed by the lift off process. This problem may be reduced by adjusting the positioning of the sample in the evaporation system.

3.2. Optical Measurements

The transmission spectra of the square arrays of holes were performed using an Optical Spectrum Analyzer (OSA) model YOKOGAWA AQ-6315A and a white light source (model Advantest

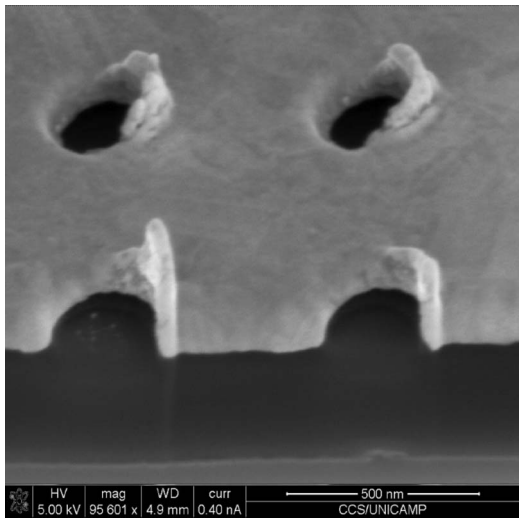

Fig. 6. SEM high resolution image of the IL sample exhibiting the details of the Au burr around the holes.

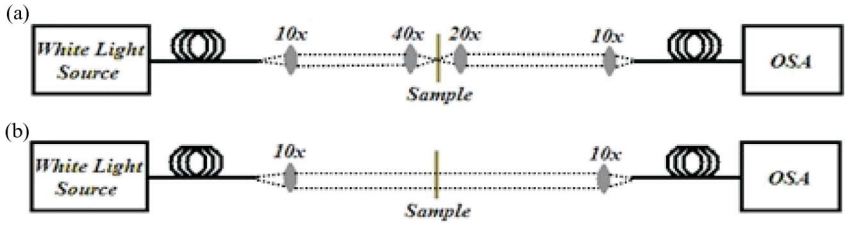

Fig. 7. Scheme of the setup used for the optical measurement (a) using a focused beam in the hole array region of the sample (about 20 μm $\times$ 20 μm) and (b) using a collimated beam into a region of about 5 mm $\times$ 5 mm of the sample.

TQ8111). Fig. 7 shows a schematic drawing of the setup used for the measurement at two different conditions of incidence: (a) focused light and collimated light. Because of the small size, the FIB samples can be measured only under focused light while the IL samples were measured using both focused and collimated light.

For comparison, Fig. 8 shows the measured transmittance spectra of both FIB and IL samples measured using the incident light focused at the same area of the samples [using the setup of Fig. 7(a)].

The peaks, marked by bars, correspond to the excitation of the first Surface Plasmon mode [$i = 1$, $j = 0$ in (5)], at the two interfaces: Au-air and Au-substrate [10], [18]. The longest wavelength peak $(1, 0)_{\text{subs}}$ is the best defined peak in both samples. For the FIB sample the $(1, 0)_{\text{subs}}$ peak is wider and red shifted in comparison to the corresponding peak for the IL sample. These effects occur because both the average period and the hole diameter of the FIB sample are larger than those corresponding of the IL sample [1], [7]. By comparing the $(1, 0)_{\text{air}}$ peaks of both samples, we observe a worse definition of this peak for the IL sample. This fact may be attributed to the burrs on the edges of the holes of the IL samples that produce larger light scattering at shorter wavelengths. On the other hand, the FIB samples present a strong conical etching of the substrate that decreases the effective refractive index of the substrate. This conical etching produces also a variation of the hole diameter along the depth of the Au film of about 15% (that is not accounted for in the 6% of variation measured from the top view images). These fabrication errors of the FIB technique may also change the plasmonic peaks positions, as well as their definition.

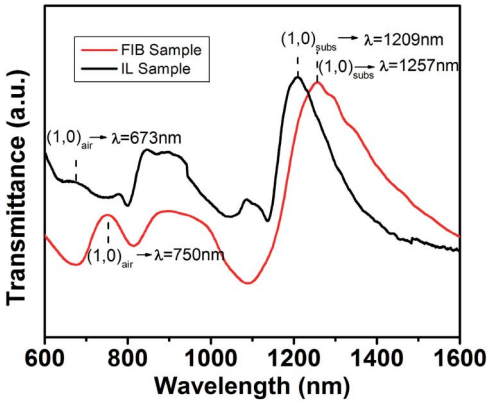

Fig. 8. Transmission spectra of FIB and IL sample obtained using focused light at the same area of the sample.

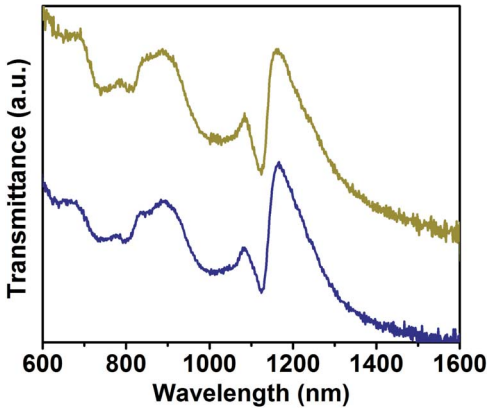

Fig. 9. Transmission spectra of different areas of the same IL sample obtained using focused light. For comparison purposes the spectra were shifted vertically.

3.2.1. Optical Measurements at Different Positions of the IL Samples

In order to check the homogeneity of the IL samples several measurements were performed in different points of the 8 mm $\times$ 8 mm samples using the same focused setup of Fig. 7(a). Fig. 9 shows two typical spectra obtained from different areas of the same sample separated of about 4 mm. Note the good agreement in both the position and the shape of the peaks between the two spectra.

3.2.2. Optical Measurements of IL Sample Using Focused $\times$ Collimated Light

In order to study the effect of collimation of the incident light we have performed measurements of the same IL sample using focused and collimated light (using the setups shown in Fig. 7(a) and (b), respectively). Fig. 10 shows the measured spectra using these two conditions. As can be seen, the spectra using collimated light present a much higher resolution in the plasmonic peaks. For the $(1,0)_{\text{subs}}$ peak there is a reduction in the full width at half maximum value by a factor of 3, and there is an increase of the peak intensity by a factor of 4. The worse resolution for focused light can be explained by the fact that in this case the components of the incident light wave-vector parallel to the metal surface [$(\vec{k}_{//})$, (1) and (3)] are not negligible, producing variations at the wavelengths of the SP resonances [given by (5)] around λ_0.

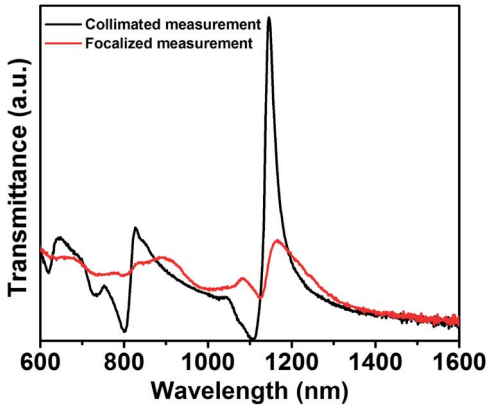

Fig. 10. Transmission spectra of IL sample measured using focused light and collimated light.

4. Conclusion

We have fabricated plasmonic arrays of holes in gold films of 100 nm of thickness with approximately the same period and hole diameter using two different techniques: IL and FIB.

The measurements of the top view SEM micrographs of the samples shown a variation in the hole diameter of about 6.5% in an area of 18 μm $\times$ 18 μm for the FIB sample and a variation of the hole diameter of 5.5% in an area of 8 mm $\times$ 8 mm, for the IL sample.

The transmittance measurements of both types of samples exhibit the characteristic SPR corresponding to the two dielectric interfaces (Au-air and Au-substrate). The intrinsic fabrication errors and characteristics of the samples recorded by each technique, however, may affect differently the optical spectra. For the measurements using focused light the FIB samples present a better definition of the plasmonic peaks at smaller wavelengths. On the other hand the large area of the IL samples allows measurements using collimated light that result in a much higher resolution of the plasmonic peaks along the all spectra. This fact allied with the lower costs of the IL makes such technique a cost-effective and high-throughput approach to nanofabrication of hole-arrays, particularly for large area devices.

Acknowledgment

The FIB work was performed at the Center for Semiconductor Components at UNICAMP. Thanks to C. Valsecchi for the support given.

References

[1] T. W. Ebbesen, H. J. Lezec, H. F. Ghaemi, T. Thio, and P. A. Wolff, "Extraordinary optical transmission through subwavelength hole arrays," *Nature*, vol. 391, no. 6668, pp. 667–669, Feb. 1998.
[2] F. J. Garcia-Vidal, L. Martin-Moreno, T. W. Ebbesen, and L. Kuipers, "Light passing through subwavelength apertures," *Rev. Mod. Phys.*, vol. 82, no. 1, pp. 729–787, Jan.–Mar. 2010.
[3] A. Lesuffleur, H. Im, N. C. Lindquist, and S. Oh, "Periodic nanohole arrays with shape-enhanced plasmon resonance as real-time biosensors," *Appl. Phys. Lett.*, vol. 90, no. 24, p. 243110, Jun. 2007.
[4] L. K. S. Kumar and R. Gordon, "Overlapping double-hole nanostructure in a metal film for localized field enhancement," *IEEE J. Sel. Topics Quantum Electron.*, vol. 12, no. 6, pp. 1228–1232, Nov./Dec. 2006.
[5] H. W. Gao, J. Henzie, and T. W. Odom, "Direct evidence for surface plasmon-mediated enhanced light transmission through metallic nanohole arrays," *Nano Lett.*, vol. 6, no. 9, pp. 2104–2108, Sep. 2006.
[6] K. J. Klein Koerkamp, S. Enoch, F. B. Segerink, N. F. van Hulst, and L. Kuipers, "Strong influence of hole shape on extraordinary transmission through periodic arrays of subwavelength holes," *Phys. Rev. Lett.*, vol. 92, no. 18, p. 183 901, May 2004.
[7] K. L. Van der Molen, F. B. Segerink, N. F. Van Hulst, and L. Kuipers, "Influence of hole size on the extraordinary transmission through subwavelength hole arrays," *Appl. Phys. Lett.*, vol. 85, no. 19, p. 4316, Nov. 2004.
[8] L. Martín-Moreno, F. J. García-Vidal, H. J. Lezec, K. M. Pellerin, T. Thio, J. B. Pendry, and T. W. Ebbesen, "Theory of extraordinary optical transmission through subwavelength hole arrays," *Phys. Rev. Lett.*, vol. 86, no. 6, pp. 1114–1117, Feb. 2001.

[9] A. Lesuffleur, H. Im, N. C. Lindquist, K. S. Lim, and S. Oh, "Laser-illuminated nanohole arrays for multiplex plasmonic microarray sensing," *Opt. Exp.*, vol. 16, no. 1, pp. 219–224, Jan. 2008.
[10] J. M. McMahon, J. Henzie, T. W. Odom, G. C. Schatz, and S. K. Gray, "Tailoring the sensing capabilities of nanohole arrays in gold films with Rayleigh anomaly-surface plasmon polaritons," *Opt. Exp.*, vol. 15, no. 26, pp. 18 119–18 129, Dec. 2007.
[11] J. A. Schuller, E. S. Barnard, W. Cai, Y. C. Jun, J. S. White, and M. L. Brongersma, "Plasmonics for extreme light concentration and manipulation," *Nat. Mater.*, vol. 9, no. 3, pp. 193–204, Mar. 2010.
[12] A. Lesuffleur, L. K. S. Kumar, A. G. Brolo, K. L. Kavanagh, and R. Gordon, "Apex-enhanced Raman spectroscopy using double-hole arrays in a gold film," *J. Phys. Chem. C*, vol. 111, no. 6, pp. 2347–2350, Feb. 2007.
[13] H. A. Atwater and A. Polman, "Plasmonics for improved photovoltaic devices," *Nat. Mater.*, vol. 9, no. 3, pp. 205–213, Mar. 2010.
[14] N. Félidj, J. Aubard, G. Lévi, J. R. Krenn, A. Hohenau, G. Schider, A. Leitner, and F. R. Aussenegg, "Optimized surface-enhanced Raman scattering on gold nanoparticle arrays," *Appl. Phys. Lett.*, vol. 82, no. 18, p. 3095, May 2003.
[15] M. J. K. Klein, M. Guillaume, B. Wenger, L. A. Dunbar, J. Brugger, H. Heinzelmann, and R. Pugin, "Inexpensive and fast wafer-scale fabrication of nanohole arrays in thin gold films for plasmonics," *Nanotechnol.*, vol. 21, no. 20, p. 205 301, May 2010.
[16] J. Chen, J. Shi, D. Decanini, E. Cambril, Y. Chen, and A.-M. Haghiri-Gosnet, "Gold nanohole arrays for bio-chemical sensing fabricated by soft UV nanoimprint lithography," *Microelectron. Eng.*, vol. 86, no. 4–6, pp. 632–635, Apr.–Jun. 2009.
[17] H. Im, S. H. Lee, N. J. Wittenberg, T. W. Johnson, N. C. Lindquist, P. Nagpal, D. J. Norris, and S. Oh, "Template-stripped smooth Ag nanohole arrays with silica shells for surface plasmon resonance biosensing," *ACS Nano*, vol. 5, no. 8, pp. 6244–6253, Aug. 2011.
[18] A. Krishnan, T. Thio, T. J. Kim, H. J. Lezec, T. W. Ebbesen, P. A. Wolff, J. Pendry, L. Martin-Moreno, and F. J. Garcia-Vidal, "Evanescently coupled resonance in surface plasmon enhanced transmission," *Opt. Commun.*, vol. 200, no. 1–6, pp. 1–7, Dec. 2001.
[19] A. Dhawan, J. F. Muth, D. N. Leonard, M. D. Gerhold, J. Gleeson, T. Vo-Dinh, and P. E. Russel, "Focused in beam fabrication of metallic nanostructures on end faces of optical fibers for chemical sensing applications," *J. Vac. Sci. Technol. B, Microelectron. Nanometer Struct.*, vol. 26, no. 6, pp. 2168–2173, Nov. 2008.
[20] S. R. J. Brueck, "Optical and interferometric lithography–Nanotechnology enablers," *Proc. IEEE*, vol. 93, no. 10, pp. 1704–1721, Oct. 2005.
[21] N. D. Lai, W. P. Liang, J. H. Lin, C. C. Hsu, and C. H. Lin, "Fabrication of two- and three-dimensional periodic structures by multi-exposure of two-beam interference technique," *Opt. Exp.*, vol. 13, no. 23, pp. 9605–9611, Nov. 2005.
[22] J. W. Menezes, J. Ferreira, M. J. L. Santos, L. Cescato, and A. G. Brolo, "Large-area fabrication of periodic arrays of nanoholes in metal films and their application in biosensing and plasmonic-enhanced photovoltaics," *Adv. Funct. Mater.* , vol. 20, no. 22, pp. 3918–3924, Nov. 2010.
[23] F. Vallini, D. S. L. Figueira, P. F. Jarschel, L. A. M. Barea, A. A. G. Von Zuben, and N. C. Frateschi, "Effects of Ga+ milling on InGaAsP quantum well laser with mirrors milled by focused ion beam," *J. Vac. Sci. Technol. B, Microelectron. Nanometer Struct.*, vol. 27, no. 5, pp. L25–L27, Sep. 2009.
[24] L. A. M. Barea, F. Vallini, A. R. Vaz, J. R. Mialichi, and N. C. Frateschi, "Low-roughness active microdisk resonators fabricated by focused ion beam," *J. Vac. Sci. Technol. B, Microelectron. Nanometer Struct.*, vol. 27, no. 6, pp. 2979–2981, Nov. 2009.